Open

Oncogene (2012) 1 – 12

www.nature.com/onc

ORIGINAL ARTICLE

Increased invasiveness of MMP-9-deficient tumors in two mouse models of neuroendocrine tumorigenesis

K Shchors[1,2], H Nozawa[3], J Xu[2], F Rostker[2], L Swigart-Brown[2], G Evan[2,4] and D Hanahan[1,3]

Despite their apparent success in pre-clinical trials, metalloproteinase (MMP) inhibitors proved to be inefficacious in clinical settings. In an effort to understand the underlying causes of this unanticipated outcome, we modeled the consequences of long-term MMP inhibition by removing one of the major players in tumorigenesis, MMP9, in two complimentary mouse models of pancreatic neuroendocrine carcinogenesis: *Myc;BclXl* and *RIP1-Tag2*. By employing gel zymography and a fluoregenic solution assay, we first established that MMP9 is expressed and activated in *Myc;BclXl* tumors in an interleukin-1β-dependent manner. The genetic deletion of MMP9 in *Myc;BclXl* mice impairs tumor angiogenesis and growth analogous to its absence in the *RIP1-Tag2* model. Notably, tumors that developed in the context of MMP9-deficient backgrounds in both models were markedly more invasive than their typical wild-type counterparts, and expressed elevated levels of pro-invasive cysteine cathepsin B. The increased invasion of MMP9-deficient tumors was associated with a switch in the spectrum of inflammatory cells at the tumor margins, involving homing of previously undetected, cathepsin-B expressing CD11b;Gr1-positive cells to the invasive fronts. Thus, plasticity in the tumor inflammatory compartment is partially responsible for changes in the expression pattern of tumor-associated proteases, and may contribute to the compensatory effects observed on MMP inhibition, hence accounting for the heightened tumor progression described in late stage clinical trials.

Oncogene advance online publication, 5 March 2012; doi:10.1038/onc.2012.60

Keywords: tumor; metalloproteinase; invasion; cathepsin; Myc; interleukin-1β

INTRODUCTION

Matrix metalloproteinases (MMPs) are a family of zinc-dependent proteinases that contribute to development and tissue homeostasis, and modulate cancer progression by digesting a variety of substrates. Owing to the role of MMP in extracellular matrix (ECM) re-arrangement (also referred to as remodeling or degradation), and in the promotion of neoangiogenesis, it was anticipated that MMP inhibition *in vivo* would have an anti-tumorigenic effect. However, phase III clinical trials with an MMP inhibitor (MMPI), combined with standard-of-care chemotherapy, failed to demonstrate clinical benefit for late stage cancer patients and, remarkably, was in some cases worse than the chemotherapy-only control arm. For instance, the use of Bay 12-9566 in treating patients with pancreatic cancer reduced both median progression-free survival and quality-of-life when compared with standard care gemcitabine.[1] In another case, treatment of glioblastoma patients rendered no statistically significant survival benefits.[2] Additionally, the clinical trials in small-cell lung carcinomas had to be terminated prematurely.[3] This failure led to the early cessation of ongoing trials, and to reconsideration of the merit of a variety of MMPIs in clinical development by a number of pharmaceutical companies.[4–6] The molecular mechanism behind this disappointing outcome of MMP inhibition is still unclear, given the demonstrable efficacy of MMPI in pre-clinical trials. The goal of this study was to look for clues that might help explain the clinical failure of MMPI.

Among candidate family members, we chose to focus on MMP9. In humans, elevated levels of MMP9 expression and its proteolytic activity correlate with poor prognosis in patients with various types of cancer.[7–9] Historically, increased MMP9 expression was viewed as a factor promoting tumor invasion.[10–12] Subsequently, MMP9 was characterized as a potent trigger of angiogenic switch in the genetically engineered mouse model of pancreatic neuroendocrine carcinogenesis, *RIP1-Tag2 (RT2)*.[13,14] The pro-angiogenic capacity of MMP9 has also been observed in other genetically engineered mouse models, including models of cervical cancer,[15,16] gliomagenesis,[17] neuroblastoma[18] and colorectal cancer.[19] Both genetic ablation and pharmacological inhibitors have been used to establish the role of MMP-9 in tumor angiogenesis. Herein, we studied the effects of long-term genetic deletion of MMP9 in two independent models of pancreatic neuroendocrine tumorigenesis (PNETs)–*RT2* and *pIns-MycER^{TAM}RIP7-Bcl-x$_L$* (*Myc;BclXl*). The use of a gene knockout of MMP-9 enabled us to avoid the complexities of pharmacological agents, such as multiple targets, incomplete inhibition and toxicity. We have previously characterized the angiogenic phenotype in both the *Myc;BclXl*[20,21] and the *RIP-Tag2* models.[13,22,23] Interestingly, the characteristics of tumor angiogenesis in the *Myc;BclXl* model, such as the release of sequestered vascular endothelial growth factor (VEGF)-A to render it bioavailable to its receptors on endothelial cells, are similar to those in the *RT2* PNET model, suggesting that the regulation of tumor angiogenesis during neuroendocrine tumorigenesis is independent of initiating lesion. However, the contributing role, if any, of MMP9 in the angiogenic phenotype of Myc-driven insulinomas has not been established yet.

[1]Swiss Institute for Experimental Cancer Research, School of Life Sciences, Swiss Federal Institute of Technology Lausanne (EPFL), Lausanne, Switzerland; [2]Department of Pathology, University of California San Francisco (UCSF), San Francisco, CA, USA and [3]Department of Biochemistry and Biophysics, University of California San Francisco (UCSF), San Francisco, CA, USA; [4]Current address: Department of Biochemistry, Tennis Court Road, University of Cambridge, Cambridge CB2 1GA, UK. Correspondence: Dr K Shchors, The Swiss Institute for Experimental Cancer Research (ISREC), School of Life Sciences, Swiss Federal Institute of Technology Lausanne (EPFL), SV2818, Station 19, CH-1015, Lausanne, Switzerland. E-mail: ksenya.shchors@epfl.ch
Received 24 July 2011; revised 17 January 2012; accepted 24 January 2012

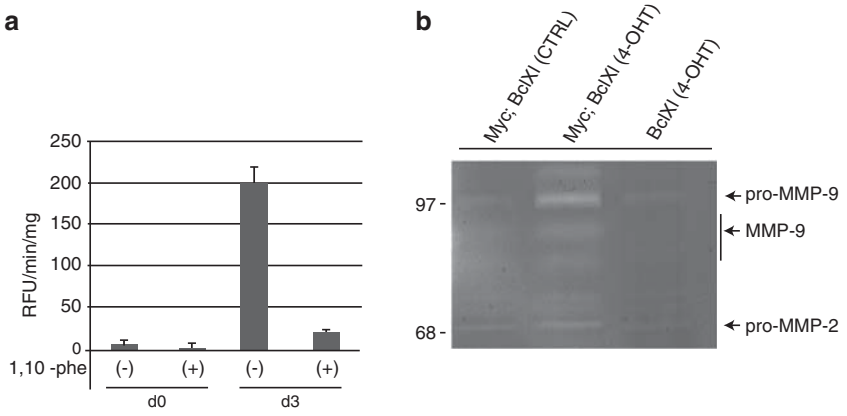

Figure 1. MMP9 is rapidly induced and activated in response to c-Myc. (**a**) Total gelatinase/collagenase activity (relative fluorescence units, RFU) in the islets of *Myc;BclXl* animals untreated (d0) or Myc ON for 3 days (three mice per experimental group), as assessed by fluorogenic solution assay utilizing quenched DQ-gelatin. Incubation of lysates with 1,10-phenanthroline (1,10-Phe) (+ , 4.0 μm) eliminated cleavage of the fluorogenic substrate. Data reflect mean ± s.e.m. (**b**) MMP9 activity was further visualized by gelatin zymogram assay. Protein lysates from control *Myc;BclXl* islets, 24-h-treated *Myc;BclXl* islets or 24-h-treated *BclXl* islets were analyzed (three mice per experimental group). Cleared region of gel indicating the presence of proMMP9, MMP9 and proMMP2 are shown.

We first showed that MMP9 is expressed and functional during the early stages of tumorigenesis in the *Myc;BclXl* model, and then proceeded to investigate in further depth the characteristics of tumors that have developed in the absence of MMP9 activity. MMP9 deficiency in the *Myc;BclXl* model had a negative impact on angiogenic switching during the initial stages of tumor progression, consistent with anti-angiogenic features of MMP9 deficiency in the *RT2* model. The advanced neoplastic lesions formed in MMP9-deficient animals in the *Myc;BclXl* and *RT2* PNET models, however, exhibited a profoundly invasive phenotype. A distinct spectrum of inflammatory cells was found at the invasive margins of MMP9-deficient tumors in comparison with wild-type counterparts, involving the emergence of a sub-population of CD11b; Gr1-positive cells that are characterized by the production of pro-invasive cysteine cathepsin B.

RESULTS

MMP9 is rapidly induced and activated in response to c-Myc

The *Myc;BclXl* model of PNET, where 4-OHT-inducible c-Myc expression is targeted to the β-cell compartment of pancreatic islets, enables the different stages of tumorigenesis to be carefully dissected. Myc is synchronously activated within 1–2 h in all β cells following systemic administration of 4-OHT.[20] To establish whether MMP9 is present and functional during the early stages of tumorigenesis in the *Myc;BclXl* model, we first determined, using a fluorogenic solution assay, that daily activation of Myc for 3 days induces MMP activity in islet tissue lysates (Figure 1a).

The analysis of a β-cell Myc target gene database obtained by laser capture microdissection and mRNA profiling of *Myc;BclXl* islets following 2, 8 and 24 h of Myc activation revealed that genes encoding candidate MMPs (MMP2, MMP3 and MMP9) are not direct transcriptional targets of Myc (Lawlor *et al*.[24] and Supplementary Figure 1a). However, MMP9 protease activity was rapidly induced in islet tissue following Myc activation *in vivo* (Figure 1a and Supplementary Figure 1b). The islets purified from *Myc;BclXl* or *BclXl* animals treated *in vivo* with control vehicle and 4-OHT for 24 h (Myc-ON) were analyzed by gelatin zymography. The induction of bands representing active and latent forms of MMP9 was detected as early as 24 h following Myc induction. The MMP9 origin of cleared regions on gelatin zymography gels was confirmed by comparing the activity profile of treated *Myc;BclXl* islets with the mobility of recombinant MMP9, and islets purified from animals deficient for MMP9 activity (Supplementary Figure 1b). We did not observe any induction of proMMP2 or activation of MMP2 (Figure 1b). Thus, despite the evidence that Myc does not directly regulate transcription and production of MMP9 in the Myc-expressing cancer cells, MMP9 induction in islets was Myc dependent. In light of multiple studies, including in *RT2*, which documented MMP9 expression by infiltrating immune inflammatory cells,[13,15] we assessed the possibility that MMP9 was also supplied by innate immune cells in the *Myc;BclXl* model.

Myc induces MMP9 in leukocytes in an interleukin-1-β-dependent manner

To determine the source of MMP9 production in neoplastic islet tissue, we treated the *Myc;BclXl* animals for 3 or 7 days with 4-OHT (Myc-ON), or control vehicle for 7 days, and analyzed tissue by immunohistochemistry for MMP9 expression. Following activation of Myc, MMP9 was increased in a subset of cells in the neoplastic tissue (Figure 2a). Immunohistochemical analysis using the leukocyte-specific marker CD45 confirmed that the CD45 + cell population is the source of MMP9 in this model (Figure 2b). Although both CD68− and F4/80-positive cells were present in abundance in islets in early stages of tumorigenesis, the majority remained negative for MMP9 production (Supplementary Figure 2). Previous immunohistological examination suggested that both CD68 + and Gr1 + populations of the inflammatory compartment of similar PNET tumors in the *RT2* model express MMP9, with the highest level of MMP9 expression associated with Gr1-positivity. Similarly, the MMP9-expressing cells inside neoplastic lesions driven by Myc are Gr1 positive (Figure 2c).

We previously demonstrated that the pro-inflammatory cytokine interleukin (IL)-1β is rapidly upregulated and secreted in the *Myc;BclXL* model.[21] As IL-1β is known to recruit inflammatory cells to tumor site,[25] we reasoned that it might be involved in recruiting and/or inducing the MMP9-expressing CD45 + leukocytes in the *Myc;BclXL* model. We therefore performed gelatin zymograms on neoplastic islets purified from *Myc;BclXl* animals subjected to Myc-activation, in conjunction with control or IL-1β neutralizing antibodies *in vivo*. Indeed, inhibition of IL-1β activity reduced Myc-mediated induction of MMP9 (Figure 2d). Moreover, immunohistochemical analysis using MMP9-specific antibodies in *Myc;BclXl* pancreas *in vivo* confirmed that MMP9 expression was dependent on IL-1β activity. The treatment of *Myc;BclXl* animals with 4-OHT (Myc ON) for 3 and 7 days combined with IL-1β neutralizing antibodies resulted in a lack of induction of MMP9

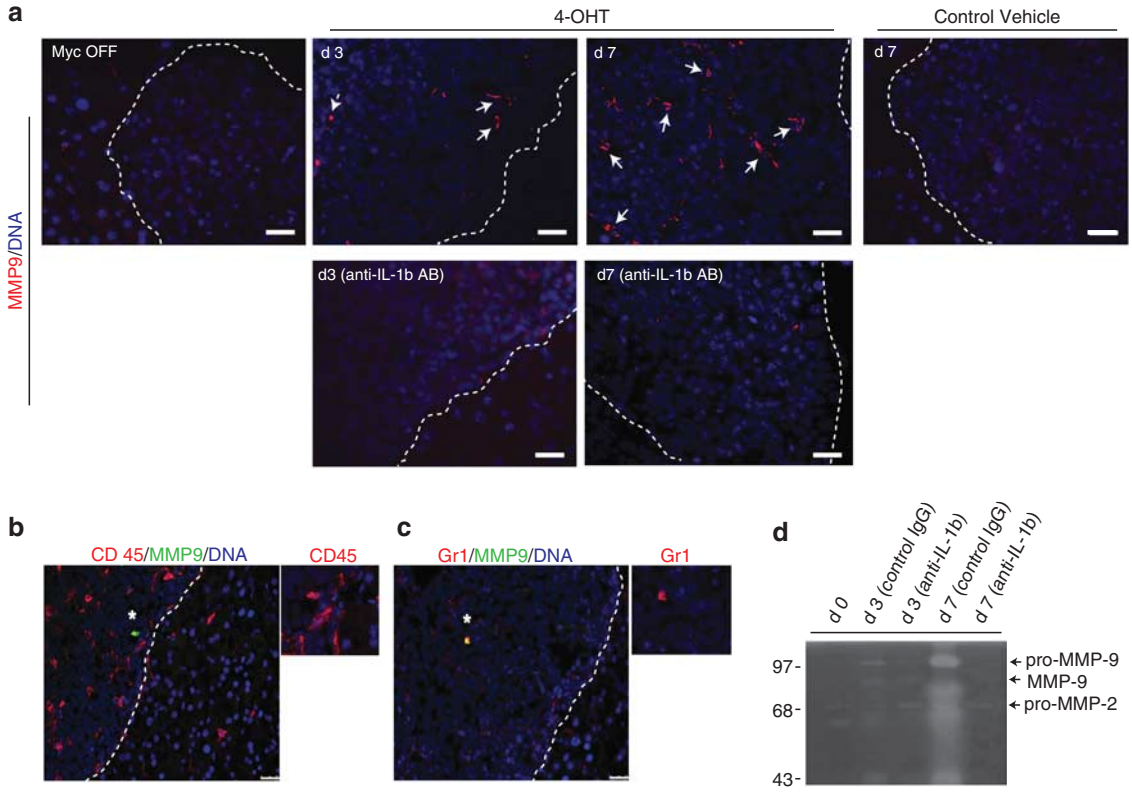

Figure 2. Myc induces MMP9 in IL-1β-dependent manner. (**a**) Pancreata were harvested from the *Myc;BclXl* mice treated for either 3 or 7 days with 4-OHT alone or in conjunction with AB-401-NA antibody (anti-IL-1β AB). For a Myc-negative control, mice were untreated (Myc OFF) or treated with control vehicle in place of 4-OHT for 7 days. Bars, 20 μm. The panels are representatives of at least three animals assayed at each data point, all analyses were done in duplicate; eight randomized fields per analysis were considered. (**b**, **c**) Immunohistochemical analysis for MMP9 expression (green) in CD45-positive (**b**) or Gr1-positive (**c**) cells in tumor tissues from *Myc;BclXl* animals treated with 4-OHT daily for 3 days. The panels are representatives of three animals. Immunohistochemical analyses done in duplicate; 12 randomized fields per analysis were considered. The tumor area is indicated by dotted line. The asterisks indicate the enlarged areas of the image. Bars, 25 μm. (**d**) Gelatin zymogram assay for MMP activity in the *Myc;BclXl* islets collected from animals untreated (d0) or treated with 4-OHT in conjunction with control (control IgG) or IL-1β neutralizing antibodies (anti-IL-1β) for the time specified (three mice per experimental group). Cleared region of gel indicating the presence of proMMP9, MMP9 and proMMP2 are shown.

expression *in vivo* (Figure 2a). We conclude that MMP9 in the *Myc;BclXl* model of carcinogenesis is provided by the inflammatory cells and depends on Myc-induced IL-1β.

Loss of MMP9 activity affects the onset of angiogenesis

As IL-1β promotes Myc-induced angiogenesis by releasing ECM-bound VEGF-A,[21] it is plausible that MMP9, being a target of IL-1β activity, is an intermediate effector of this process. To address this possibility, we first determined whether inhibition of MMP activity affects Myc-induced VEGF-A release by *Myc;BclXl* islets. VEGF-A levels were determined by enzyme-linked immunosorbent assay in a medium conditioned by *Myc;BclXl* islets cultured *in vitro* with control vehicle or 4-OHT for 3 days in conjunction with control vehicle (dimethylsulphoxide) or a pan-MMPI (GM6001). Indeed, Myc-induced VEGF-A release by islets was compromised by MMP inhibition *in vitro* (Figure 3a).

To determine the biological significance of MMP9 regulation of VEGF-A levels *in vivo*, *Myc;BclXl* animals were crossed with *MMP9*-deficient animals. The resulting *Myc;BclX:MMP9*$^{-/-}$ and *Myc;BclXl;MMP9*$^{+/+}$ animals were treated with 4-OHT for 3 days (Myc-ON). We previously demonstrated that endothelial cells in *Myc;BclXl* islets start proliferating as early as 2 days following c-Myc activation *in vivo*;[21] thus 72 h of Myc activation is an appropriate time point to follow Myc-induced angiogenesis. The proliferative status of the endothelial compartment in isolated pancreatic islets was determined by analyzing co-expression of Meca-32 (an endothelial cell-specific marker) and Ki67 (a proliferation marker). We observed a delay in onset of angiogenesis in MMP9-null animals compared with *MMP9*$^{+/+}$ (Figure 3b) and MMP9$^{+/-}$ littermates (not shown). We next assessed VEGF localization in the Myc-OFF pancreata vs pancreata collected from the animals following Myc activation for 3 and 7 days. Although VEGF-A in *Myc;BclXl;MMP9*$^{+/+}$ animals was released en mass from the ECM of pancreatic islets and associated with the islet vessels, as demonstrated by its colocalization with Meca-32 (yellow staining in panels v and vi, Figure 3c), a substantial amount of VEGF-A in MMP9-deficient islets was still associated with ECM and not with the endothelium (red staining in panels ii and iii, Figure 3c), much like in normal islets (Myc-OFF islets, panels i and iv). The specificity of VEGF-A antibodies was confirmed by immunohistochemical analysis of *RT2;RipCRE;VEGFAFlox/Flox* pancreata that lack expression of VEGF-A in islets (Figure 3c).[23] Our data suggest that blood vessel formation in MMP9-deficient tumors differs in its characteristics from wild type, and is likely to be less dependent on VEGF-A activity.

Loss of MMP9 activity promotes tumor invasion

Having established that MMP9 activity and involvement in VEGF bioavailability is similar between *Myc;BclXl* and *RT2* tumors, we proceeded to investigate whether MMP9 activity affects tumor progression. We first focused on Myc-driven tumorigenesis. The

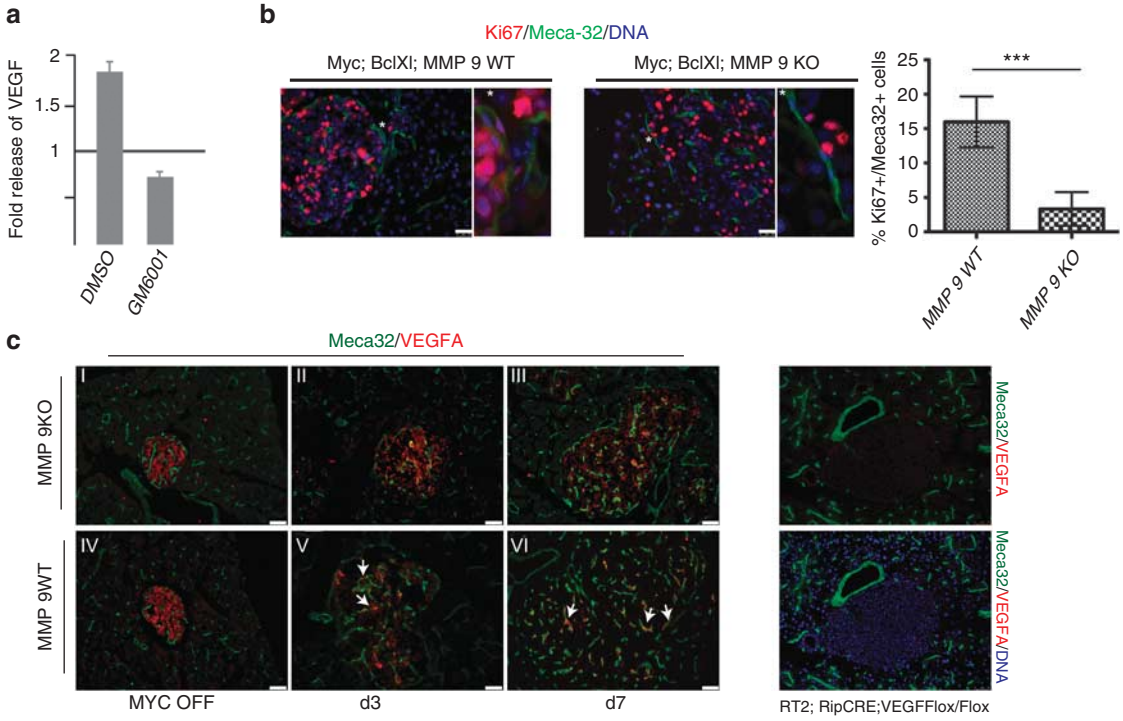

Figure 3. Loss of MMP9 activity affects onset of angiogenesis. (**a**) The pan-MMPI (GM6001) blocks Myc-induced release of VEGF from islets *in vitro*. The islets isolated from the *Myc;BclXl* animals were treated *in vitro* with control vehicle or 4-OHT for 3 days in conjunction with control vehicle (dimethylsulphoxide) or GM6001. Culture media were then collected, and VEGF-A levels were assayed by enzyme-linked immunosorbent assay. The bars show VEGF-A induction by 4-OHT relative to samples treated with ethanol for 72 h. The data are representative of three independent experiments. (**b**) Immunohistochemical analysis of endothelial proliferation *in vivo*. The *Myc;BclXl* animals from MMP9-deficient or MMP9 wild-type backgrounds were treated with 4-OHT for 3 days. Pancreata was isolated and analyzed by immunohistochemistry (IHC). Proliferating endothelial cells were identified by co-labeling with the endothelial marker Meca-32 (green) and Ki67 (red); nuclei are visualized with Hoechst dye (blue). The endothelial compartment of islets is indicated by asterisks. Bars, 50 μm. The percentage of Meca-32-positive cells that also stained positive for the proliferation marker Ki67 was then determined as described in Materials and methods section. ***$P<0.0001$ by Student's *t*-test analysis. (**c**) MMP9 deficiency inhibits Myc-induced redistribution of VEGF-A in islets. The *Myc;BclXl* animals from MMP9-deficient and wild-type backgrounds were treated with 4-OHT daily. As the times indicated, animals were killed and pancreata isolated, sectioned and stained with anti-VEGF-A antibody (red) and Meca-32 (green). Areas of focal VEGF-A accumulation are indicated by arrows. Bars, 50 μm. *RT2;RipCRE;VEGF-A Flox/Flox* pancreata is provided as a control for the VEGF-A antibody specificity. The panels are representatives of at least three animals assayed at each data point, immunohistochemical analyses done in triplicate; 10 randomized fields per analysis were considered.

animals from *Myc;BclXl;MMP9KO* and control *Myc;BclXl* backgrounds were subjected to treatment with 4-OHT for 3, 7 and 21 days. Short-term Myc-activation in the *Myc;BclXl* model promotes proliferation of β cells and the associated endothelial cell compartment of pancreatic islets, while prolonged (21 days) treatment results in tumor formation.[20,21] Histopathological analysis of pancreata by hematoxylin and eosin staining revealed no gross pathological difference between control and MMP9-deficient islets in untreated and 3-day-treated samples (Supplementary Figure 3). Surprisingly, however, the *Myc;BclXl;MMP9*-deficient tumors exhibited a heightened invasive phenotype, with projections of cells extending into surrounding exocrine tissue following just 1 week of Myc activation (Supplementary Figure 3), which continued after long-term activation of Myc (Figure 4a and Supplementary Figure 3).

We then asked whether the pro-invasion phenotype of MMP9-deficient carcinomas was a selective feature of Myc-driven tumorigenesis, or a more general effect of MMP9 inhibition. Similar analysis of the consequences of MMP9 loss in the *RT2* model revealed that late stage *RT2* tumors in MMP9-deficient animals also exhibited higher levels of invasiveness than control counterparts (Figure 4b). The pancreata collected from both *Myc;BclXl* (21-day-treated, long-term treatment) and *RT2* (13 weeks, late stage tumorigenesis) animals from the $MMP9^{-/-}$ background exhibit a 30% increase in tumors with a more advanced invasion phenotype when compared with the corresponding tumors from $MMP9^{+/+}$ and $MMP9^{+/-}$ backgrounds (Figures 4c–f). Tumor invasiveness was additionally scored based on a circularity criterion. The MMP9-deficient PNETs had more irregular tumor borders than their wild-type controls as reflected by decreased circularity (Figure 4g). In contrast, advanced MMP9-deficient tumors in both models were similar to their wild-type counterparts in vascular network complexity, level of tissue hypoxia and collagen IV coverage (Supplementary Figures 4 and 5).

Tumors developed from MMP9-deficient background exhibit increased activity of cysteine cathepsin proteases

Having established that loss of functional MMP9 results in the formation of more aggressive lesions, we performed additional analysis of MMP9-deficient tumors, focusing on factors that might explain the increase in tumor invasion.

It was recently demonstrated that members of the cysteine cathepsin family promote invasion in the *RT2* model,[26] and thus were plausible candidates. We first determined whether total cathepsin activity is increased in tumors developed from MMP9-deficient backgrounds. For this purpose, protein lysates were

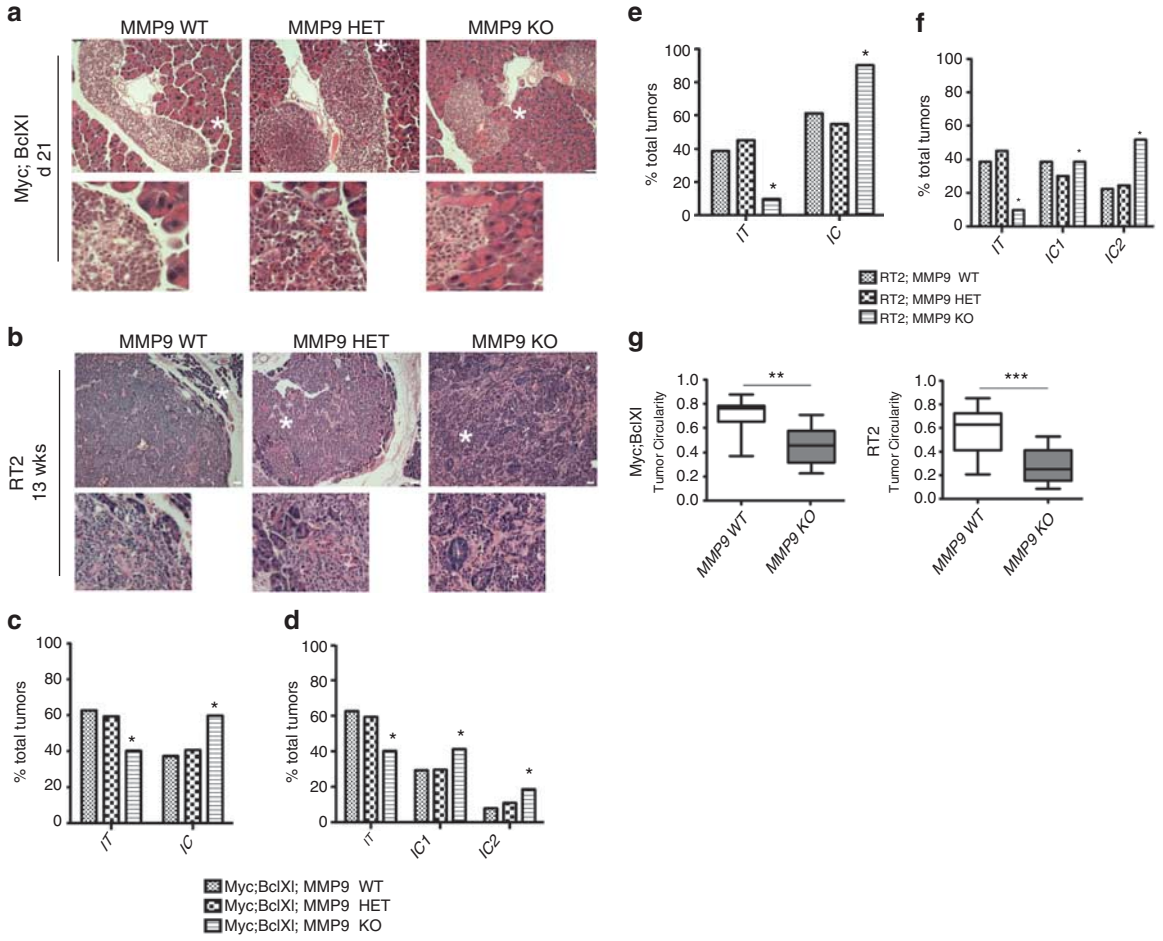

Figure 4. Loss of MMP9 activity promotes tumor invasion. Histopathological analysis by hematoxylin and eosin staining of pancreatic neurodendocrine tumors from the *Myc;BclXl* animals treated with 4-OHT daily for 21 days (**a**) and from 13-week old *RT2* animals (**b**), in both cases that were either MMP9 wild type (WT), heterozygous (HET) or genetically deficient (KO). The asterisks indicate areas of tumor tissue enlarged below. Bars, 75 μm (**a**) and 100 μm (**b**). (**c**) Quantification of tumor invasiveness represented as the percentage of IT lesions or total IC lesions (IC1 + IC2) in *Myc;BclXl* animals from different MMP9 backgrounds. A minimum of 51 tumors per group were graded. $*P \leqslant 0.02$ by Fisher's exact test. (IT, islet tumor; IC, invasive carcinomas; IC1, invasive carcinoma type 1; IC2, invasive carcinoma type 2). No statistically significant difference was observed between MMP9 WT and MMP9 HET genotypes. (**d**) Same as (**c**) except IC lesions are separated into the IC1 and IC2 subclasses. $*P < 0.01$ by the χ^2 test. (**e**) Quantification of tumor invasiveness represented as the percentage of IT lesions or total IC lesions (IC1 + IC2) in *RT2* animals from different MMP9 backgrounds. A minimum of 49 tumors per group were graded. $*P < 0.01$ by Fisher's exact test. No statistically significant difference was observed between MMP9 WT and MMP9 HET genotypes. (**f**) Same as (**e**) except IC lesions are separated into the IC1 and IC2 subclasses. $*P < 0.01$ by the χ^2 test. (**g**) Quantification of *Myc;BclXl* and *RT2* tumor circularity from MMP9 WT and MMP9 KO backgrounds. A minimum of 23 tumors per group were analyzed. $**P < 0.001$, $***P < 0.0001$ by Student's *t*-test.

prepared from freshly frozen tumor samples and incubated with a specific biotinylated cathepsin activity probe as has been described.[27] The tumors collected from MMP9-deficient backgrounds had higher levels of cathepsin activity than tumors from wild-type (Figure 5a) and $MMP9^{+/-}$ (Supplementary Figure 6) counterparts.

We next performed western blot analyses to identify members of cysteine cathepsin family that might be responsible for the increased protease activity in the MMP9-deficient samples. As cathepsins C, S and B have been identified as major contributors to tumor progression and tumor invasion,[26] we at first examined their expression. We determined that cathepsin B (Figure 5b), but not cathepsin S or cathepsin C (Figures 5c and d)–is significantly elevated in the tumors from $MMP9^{-/-}$ background.

MMP9-deficient tumors differ in their inflammatory profile

It is well established that tumor invasion can in some cases depend on the selective remodeling of ECM by proteases.[28] Most proteases involved in restructuring the ECM are supplied by the inflammatory compartment.[29] Correlation has been observed between the type of inflammatory cells and the particular secreted proteases that contribute to tumor progression.[29] As MMP9-deficient tumors are more invasive than their counterparts, we sought to determine the spectrum of inflammatory cell types in MMP9-deficient tumors.

Tumor-associated macrophages have been described as a major source of cathepsin B *in vivo*,[26] therefore we first assessed macrophage abundance using the macrophage-specific CD68 marker. Interestingly, we detected reduced numbers of CD68+ macrophages in MMP9-deficient lesions compared with wild-type tumors in both the *RT2* and *Myc;BclXl* models (Figures 6a and b). This result is consistent with prior studies demonstrating that the recruitment of macrophages can be MMP9 dependent.[18,30,31]

Depletion of macrophages provokes an influx of other leukocytes to the tumor site, whose recruitment is otherwise inhibited by specific macrophage secreted factors.[16] Therefore, we

hypothesized that, in a similar manner, stromal cells of non-monocytic lineage are predominant in MMP9-deficient tumors. To address the question, we assessed the presence of various leukocytes using cellular antigen-specific markers. We used CD3 (lymphocytes), CD4 (T-lymphocytes), Gr-1 (Ly6G-myeloid differentiation antigen, present in bone marrow granulocytes peripheral neutrophils, myeloid progenitors) and CD11b (Mac-1, mainly myeloid cells) to visualize the respective cell types in the

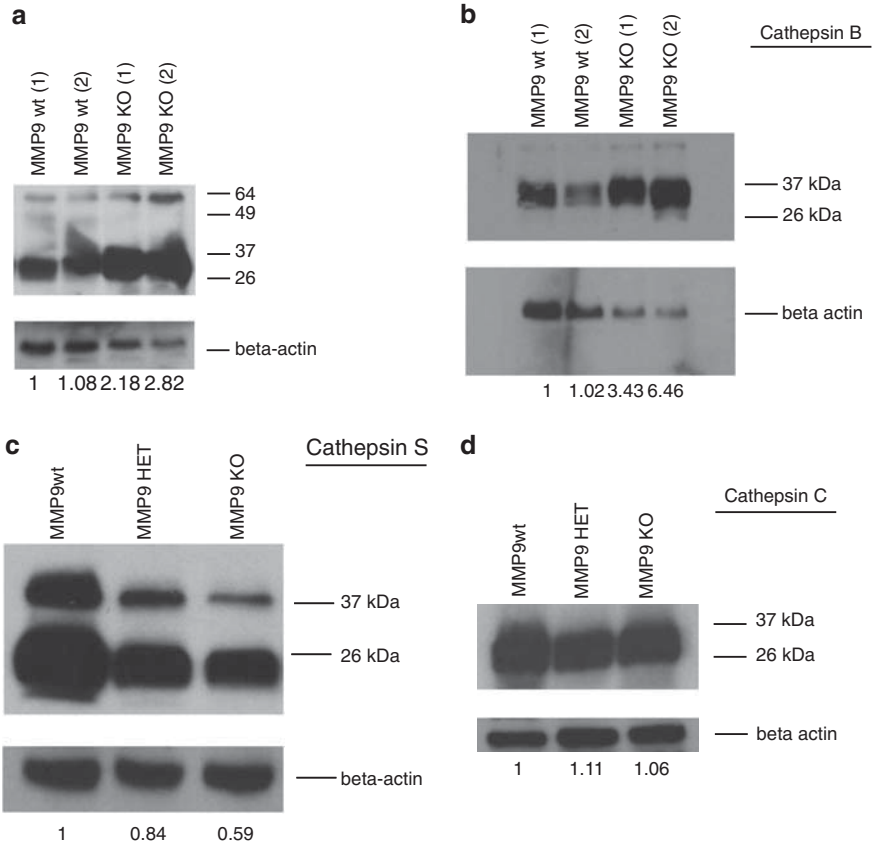

Figure 5. MMP9-deficient tumors exhibit increased cathepsin activity. (**a**) Cathepsin activity profiles for the *RT2* tumors from MMP9 wild-type (WT) and MMP9-deficient background (KO) using the biotinylated cathepsin activity probe DCG-04 ABP on tissue lysates. β-Actin was used as a loading control. The figure shows activity in two independent tumors of each genotype. Molecular weight markers are indicated on the side panel. Quantification represents expression relative to the first MMP9 WT lane. (**b**) Western blot analysis of the *RT2* MMP9 WT and MMP9 KO tumor lysates using cathepsin B-specific antibodies. β-Actin was used as a loading control. Molecular weight markers are indicated on the side panel. The figure shows activity in two independent tumors from the MMP9 WT and MMP9 KO backgrounds. Quantification represents expression relative to the first MMP9 WT lane. (**c**) Western blot analysis of the *RT2* MMP9 WT, MMP9 HET and MMP9 KO tumor lysates using cathepsin S-specific antibodies. β-Actin was used as a loading control. Molecular weight markers are indicated. Quantification represents expression relative to the MMP9 WT lane. (**d**) Western blot analysis of the *RT2* MMP9 WT, MMP9 HET and MMP9 KO tumor lysates using cathepsin C-specific antibodies. β-Actin was used as a loading control. Molecular weight markers are indicated. Quantification represents expression relative to the MMP9 WT lane.

Figure 6. MMP9-deficient tumors differ in their inflammatory profile from wild-type counterparts (**a**) Quantification of inflammatory cells recruited to the *RT2* or to the *Myc;BclXl* tumor sites in MMP9 WT (blue) and MMP9 KO (orange) backgrounds. The data quantify CD68, CD4, Gr1 and Gr1/CD11b-positive cells as a percentage of total cells in the tumor tissue. *P*-values were determined by the Student's *t*-test. **P*-value of $P \leqslant 0.01$ was considered significant. (**b**) Immunohistochemical analysis of CD68-positive cells (macrophages) in tumor tissues from the *Myc;BclXl* animals treated with 4-OHT daily for 21 days, of from 13-week old *RT2* animals, in each case in the context of MMP9 WT or MMP9 KO backgrounds. Positive cells are indicated with arrows. Bars, 25 μm. (**c**) Immunohistochemical analysis of CD4-positive cells (red, T-lymphocytes) in tumor tissues described above. Positive cells are indicated with arrows. Bars, 25 μm. (**d**) Immunohistochemical analysis of Gr1-positive cells (red, myeloid differentiation antigen, present in bone marrow granulocytes and peripheral neutrophils) in tumor tissues described above. The tumor invasion front is indicated by a dotted line. Bars, 50 μm (*RT2* tumors) and 25 μm (*Myc;BclXl*). (**e**) Representative images of Gr1 (green) and CD11b (Mac-1) (red) cells in tumor tissues from *RT2* animals of MMP9 WT and MMP9 KO backgrounds. The tumor invasion front is indicated by a dotted line. The cells of myeloid origin co-express both the markers. The asterisks indicate the area of tumor represented in the insert on a right upper corner. The insert shows staining for CD11b alone. Bars, 75 μm. (**f**) Analysis of cathepsin B expression in Gr1-positive cells in tumor tissues from the *RT2* animals in the context of MMP9 WT or MMP9 KO backgrounds. The asterisks indicate the enlarged areas of the image that show staining for cathepsin B (red) and Gr1 (green). Bars, 10 μm. (**g**) Same analyses as (**f**) performed in tumor tissues from *Myc;BclXl* animals in the context of MMP9 WT or MMP9 KO backgrounds. Bars, 25 μm. (**h**) Quantification of Gr1 + /cathepsin B + cells recruited to the *RT2* or to the *Myc;BclXl* tumor sites in MMP9 WT and MMP9 KO backgrounds. A minimum 27 tumors per group were analyzed. **One Gr1 + /cathepsin B + cell was detected in the *RT2;MMP9 WT* tumors. *No Gr1 + /cathepsin B + cells were detected in the *Myc;BclXl;MMP9 WT* tumors.

PNET tumors from MMP9$^{+/+}$ and MMP9$^{-/-}$ backgrounds. We observed a minor increase in the CD4+ fraction (Figure 6a). However, the localization of CD4+ cells in tumors did not correlate with the invasive front and, thus, these cells are unlikely to contribute to the increased invasion of MMP9-deficient lesions (Figure 6c). On the other hand, Gr-1+ cells, whose recruitment to the site of MMP9-deficient tumors was also increased (Figure 6a), were localized to the invasive front of the tumors (Figure 6d). The majority of those cells were CD11b positive, suggesting their myeloid origin (Figures 6a and e).

As pro-invasive cathepsin B was the differential factor present in MMP9-deficient tumors, we sought to determine the source of the increased cathepsin B activity. Myeloid cells are reported to express a spectrum of proteases including neutrophil elastase, a known activator of cathepsin B activity.[32,33] However, a western blot analysis for neutrophil elastase expression in MMP9-deficient tumors showed no significant induction of this protein when compared with MMP9 wt counterparts (Supplementary Figure 7a). Thus, there is no evidence linking neutrophil elastase and cathepsin B activity in our model. The major source of cathepsin

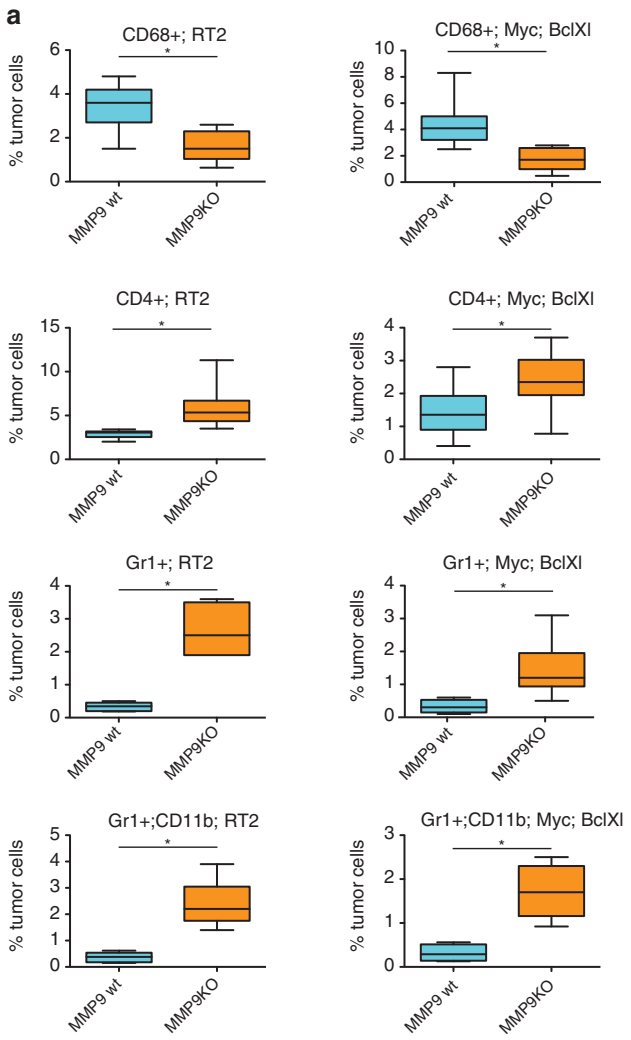

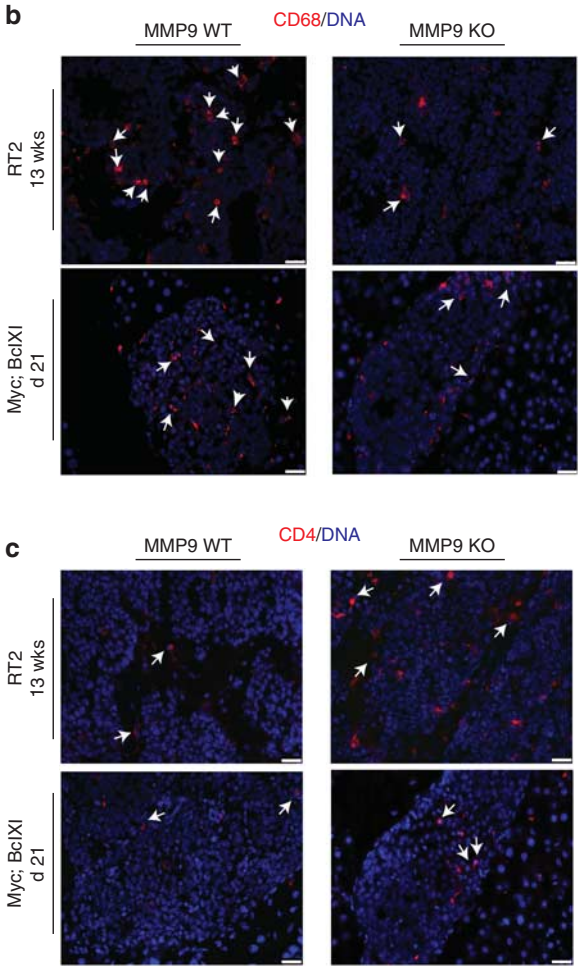

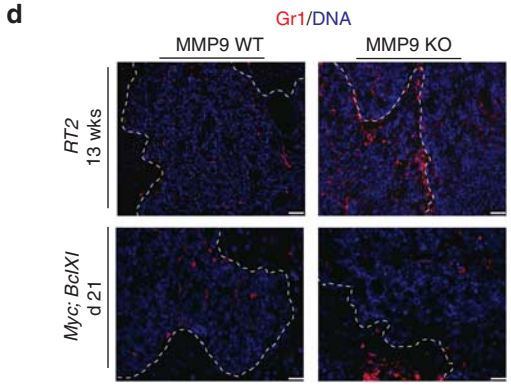

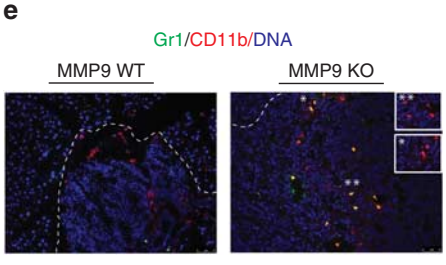

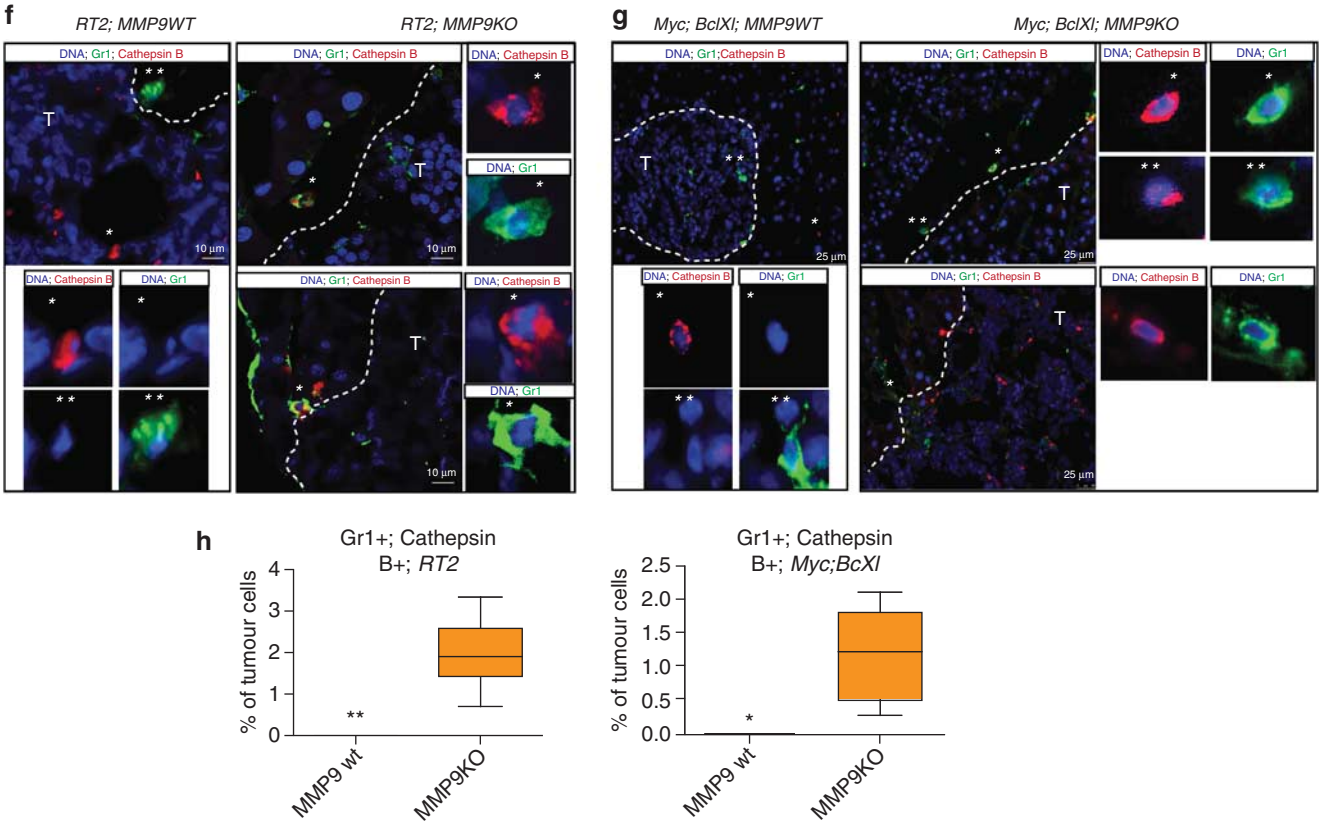

Figure 6. Continued.

B in the *RT2* model is CD68+ monocytes. Indeed, we detected CD68+ cells expressing cathepsin B in tumors from both backgrounds, but the total number of those cells was reduced in MMP9-deficient tumors (Figures 6a and b, or Supplementary Figure 7b). Gr1+ cells, which are readily detectable in tumors from both MMP9-deficient backgrounds, do not express cathepsin B in *RT2;MMP9* wt and *Myc;BclXL;MMP9* wt tumors (Gocheva *et al*.[26] and Figures 5f–h). We therefore hypothesized that a distinct subset of Gr1+ cells, recruited to the tumor site in the context of reduced macrophage abundance, becomes an alternative source of cathepsin B. Indeed, the analysis of cathepsin B expression in the Gr1+ population of MMP9-deficient tumors revealed that a majority of Gr1+ cells localized to the invasive front of the tumors were expressing cathepsin B in both *RT2* and *Myc;BclXl* tumors (Figures 6f–h). Thus, we establish that lack of MMP9 activity in two independent models of carcinogenesis promotes tumor invasion, and is associated with expression of pro-invasive cathepsin B by a sub-population of Gr1+ cells.

DISCUSSION

The failure of MMPIs in clinical trials was originally attributed to unspecific targeting, inefficacy of drugs and the redundancy of MMPs;[5,34] in addition, the MMPIs were administered at the late stages of tumor progression, when MMP activity is now known to be less critical for tumor growth.[4,5] It subsequently emerged that, along with their originally described role as regulators of ECM remodeling and facilitators of tumor growth, MMPs modulate the activity of both inducers and inhibitors of tumorigenesis, by processing cytokines, angiogenic and growth factors, and their respective receptors, as well as altering cell adhesion and stimulating epithelial to mesenchymal transition.[35]

We sought to investigate events behind inefficacy of MMP inhibition, focusing our analysis on MMP9, the key regulator of tumor angiogenesis in various tumor models including the PNET model-*RT2*.[13,17,36,37] We established that, in a complimentary model of PNET-*Myc;BclXl*-MMP9 promotes tumor angiogenesis as well. The advantage of the *Myc;BclXl* model lies in the rapid and highly synchronized onset of the disease exhibiting 'hallmarks' of cancer progression such as angiogenic switching, inflammation and invasion.[20] MMP9 expression and proteolytic activity were increased within the first days of the *Myc*-induced neoplastic progression, suggesting that this protease could be involved in the early stages of tumorigenesis. Indeed, MMP9 deficiency in the *Myc;BclXl* model had a negative effect on angiogenic switching (Figure 3b), and promoted transient tissue hypoxia (Supplementary Figure 5d). However, the advanced *Myc;BclXl;MMP9*$^{-/-}$ tumors that developed following 21 days of Myc activation were well vascularized (Supplementary Figure 5c). Concordantly, although the loss of MMP9 had a negative impact on angiogenic switch in hyperplasias and dysplasias the RT2 model,[13] the RT2;MMP9$^{-/-}$ invasive carcinomas that subsequently developed in RT2;MMP9$^{-/-}$ mice were well vascularized. The molecular mechanism by which the MMP9-deficent tumors elicit MMP9-independent angiogenesis in late stages of tumor progression is currently unclear. It is possible that transient tissue hypoxia occurring during MMP9-deficient tumor progression triggers this adaptation, for example, by recruiting cathepsin-expressing myeloid cells.[25]

The increased production and activation of MMP in tumors observed in several other models of Myc-driven tumorigenesis was attributed to the direct transcriptional regulation of MMP by Myc in cancer cells.[38–40] However, it is now well established that MMPs supplied by inflammatory cells rather than by cancer cells

themselves are major players in promoting tumorigenesis.[14,18,37] Our data indicate that signaling between tumor cells and the inflammatory compartment of the PNETs is mediated by inflammatory cytokine IL-1β. A growing body of evidence indicates that inflammatory cytokine IL-1β, which has an important role in acute and chronic inflammatory diseases, might mediate signaling between tumor and inflammatory cells.[21,41,42] IL-1β orchestrates the expression of a variety of factors including: growth factors,[43] chemoattractants[44] and matrix MMPs.[45,46] Our data suggest that IL-1β, which triggers the initial steps of Myc-induced angiogenesis, mediates production of MMP9 in the microenvironment of *Myc;BclXl* tumors. Moreover, elevated expression of IL-1β was recently observed during angiogenic switching in the *RT2* model, making IL-1β a possible candidate in promoting RT2 tumorigenesis (Sadanandam and Hanahan, unpublished).

Despite the well-established pro-angiogenic and tumor-growth-promoting role of MMP9, we found that genetic deficiency for this protease contributed to the increased invasiveness of tumors both in the *Myc;BclXl* and in the independent *RT2* models of PNET. A number of previous studies hinted that loss of MMP9 activity might render more hostile tumors. For example, in the K14-HPV16 model of squamous skin carcinogenesis, while MMP9 deficiency decreased the total number of tumors, the emerging tumors were significantly more aggressive than wt counterparts.[36] Additionally, MMP9-deficient cancer cells exhibited increased invasiveness in a glioblastoma model,[17] an effect that was also witnessed in the CR2-Tag model of prostate tumors.[37] We observed that increased invasion in the MMP9-deficient cancers was associated with the reduction of CD68+ cells, whose homing, at least in part, is mediated by MMP9 proteolytic activity (for review, see Campbell *et al*.[30] and Deryugina and Quigley[47]). Interestingly, the decreased percentage of CD68+ cells inversely correlated with the presence of CD11b+; Gr1+ cells at the tumor margins. Notably, CD11b; Gr1-positive cells have been increasingly implicated as facilitators of tumor invasion and metastasis.[48–50] There is a complex crosstalk between CD68+ and CD11b+; Gr1+ cells in tumors. For instance, in a mouse model of cervical carcinogenesis, the impaired recruitment of macrophages resulted in increased migration of neutrophils to the tumor site, because of the ablation of neutrophil inhibiting factors normally secreted by those macrophages.[16] Moreover, MMP9 deficiency in the MMTV/neu mouse model of mammary carcinoma is associated with the depletion of tumor-associated monocytes, and increased infiltration of neutrophils (Werb, personal communication).

There are currently several hypotheses aiming to explain the pro-invasive consequences of MMP inhibition. One possibility is that loss of MMP9 activity results in retention of ECM-bound VEGF. The pro-invasive and pro-metastatic potential of VEGF inhibitors was recently described.[51,52] Another is that deficiency in MMP activity in skin tumors might reduce host defense by modulating chemokines and cytokines.[53,54] Herein, we present evidence that in PNETs the loss of MMP9 activity in tumors is accompanied by a shift in the spectrum of proteases toward expression of cysteine cathepsins, specifically cathepsin B (in part supplied by CD11b; Gr1-positive cells), which may provide compensatory protease activity.

The cysteine cathepsin family, which currently consists of 11 members,[55] is predominately found inside the lysosomal compartment of the cell. Several members also are released in the extracellular space, and are involved in a variety of normal physiological processes (for review, see Turk *et al*.[56]). In addition, the abnormal expression and activity of some of the cysteine cathepsins in lesions of different origin implicates these proteases in promoting tumor progression.[57] The expression of secreted cysteine cathepsins has been associated with tumor progression in several models of carcinogenesis including K14-HPV16-driven cervical cancer,[27] K-ras^{G12D} lung adenocarcinomas,[58] *RT2* PNETs[27] and *Myc;BclXl* PNETs (Shchors and Evan, unpublished). Upregulation of six cathepsins (B, C, H, L, S and Z) was observed in the *RT2* model;[27] among them, cathepsins B and S supplied by inflammatory cells demonstrably promoted tumor invasion.[26,59] The exact mechanism by which cathepsin B contributes to invasion is still under investigation. Cathepsin B is directly involved in degradation of a variety of targets, including such ECM proteins as fibronectin, types I and IV collagen and laminin[60–62] as well as cell adhesion molecule E-cadherin.[59] Although cathepsin B is present and functional in the MMP9 competent tumors, we have now established that the spectrum of cathepsin B producing cells and the levels of cathepsin B are elevated on the loss of MMP9 activity. It was previously suggested that the source of protease expression might affect not only the levels of the enzyme *per se* but also its pro-tumorigenic activity.[8,14] For example, epithelial cancer cell versus stromal cell expression of MMP has differential prognostic correlation with overall survival in cases of epithelial ovarian cancer.[8] The MMP and cathepsin families are joined in a complicated network of protease activity in tissues (for review, see Levicar *et al*.[63]). It is apparent that MMP9 and cathepsin B differ in their pro-invasive capacity. For instance, in the analysis of gastric carcinomas, high expression of cathepsin B, but not MMP9, was a statistically significant parameter in the depth of tumor invasion.[64] Interestingly, there are some indications that success of therapeutic trials targeting MMP activity is linked to the lack of cathepsin B in the tumors. For example, inhibition of MMP activity in renal cell carcinoma, a type of cancer with exceptionally low levels of cathepsin B,[65] was one of the rare MMPI trials where the overall survival of the patients was significantly prolonged.[66] Our results are consistent with the initial observations that MMPs act mostly as regulators of tumor angiogenesis,[13,14] while cysteine cathepsins contribute to invasion potential of the tumors.[27,59] On inhibition of MMP activity, tumors can evidently highjack the existing blood supply in an organ,[17] possibly achieving the required increased migratory capacity by engaging cathepsins. Our data support a mechanism in which tumors acquire resistance to MMPIs by employing another type of protease activity, contingent on a change in the spectrum and abundance of tumor-promoting inflammatory cells and hence of the proteases they supply. In such cases, therapeutic targeting of both families of proteases might prove efficacious, by obviating the demonstrable adaptive resistance to MMPIs.

MATERIALS AND METHODS

Mice, tissue sample generation, manipulation and preparation

All mice were housed, fed and treated in accordance with protocols approved by the committee for animal research at the University of California, San Francisco, CA, USA. The RT2 mouse model of pancreatic islet cell carcinogenesis and transgenic mice expressing switchable MycER^{TAM} and constitutive Bcl-x_L in their pancreatic β cells pIns-MycER^{TAM}RIP7-Bcl-x_L (Myc;BclXl) mice have been previously described and characterized.[13,20] MycER^{TAM} was activated in β cells *in situ* by daily intraperitoneal injection of tamoxifen (TAM) (1 mg/mouse/day) dissolved in peanut oil (Sigma, St Louis, MO, USA). TAM is metabolized *in vivo* to 4-OHT and has an equivalent effect to 4-OHT when administered to Myc;BclXl mice. The MMP9-deficient animals from C57BL/6 background were kindly provided by Dr Z Werb (UCSF). Tissues were prepared as previously described for frozen and paraffin embedding.[67,21] The hematoxylin and eosin grading of tumors was performed as described.[67,68] At least 49 tumors for each genotype were analyzed. Analysis of tumor circularity was performed with the Fiji Software package (http://rsb.info.nih.gov/ij). The method is described as follows. Serial hematoxylin and eosin-stained sections of the entire pancreata from the tumor-bearing animals were scanned with a Leica DM5500 (Wetzlar, Germany) at ×20 magnification. The software then takes a manually outlined tumor border, and outputs a coefficient of circularity which varies between 0 and 1, where 1 denotes prefect circularity. At least 23 tumors for each genotype were analyzed. The

characterization of islet and tumor vasculature, and inhibition of systemic IL-1β *in vivo* were performed as described.[21]

Isolation of pancreatic islets and *in vitro* analysis

To assay VEGF-A release, the fibrinogen-embedded islets isolated from pancreata[21] were cultured for 48 h in the presence of either 100 nM 4-OHT or carrier in conjuction with pan-MMPI GM6001 (20 μM) (Chemicon, Temecula, CA, USA) or equal volume of control vehicle dimethylsulphoxide. The conditioned medium was collected and assayed for VEGF-A by Super-ELISA (Biotraces, Inc., Herndon, VA, USA) according to proprietary protocol. For substrate conversion assay or substrate zymography, the pancreata from *Myc;BclXl* and *BclXl* mice was isolated omitting digestion with collagens P and analyzed directly.

Substrate conversion assay and zymography

Freshly isolated pancreatic islets from the *Myc;BcXL* mice daily treated with 4-OHT or control vehicle for 3 days were lysed in solubilization buffer (25 mM Tris (pH 7.6), 0.25% Triton X-100, 5 mM $CaCl_2$). Protein concentration was determined by the Bio-Rad DC (Hercules, CA, USA). Substrate conversion assay and application of MMPI 1,10 phenanthroline (Sigma) was carried out as described.[69] Fluorescence measurements were performed using a microplate spectrofluorometer (SpectraMax Gemini EM, Molecular Devices, Sunnyvale, CA, USA) operated by SoftMax Pro 4.1 software. Values shown represent the mean ± s.e.m. from three independent islet isolations of analyses performed in triplicate.

Equivalent amount of protein extract was analyzed by gelatin zymography[70] on 10% sodium dodecyl sulfate (SDS)-polyacrylamide gels co-polymerase with substrate (1.2 mg/ml of gelatin) in sample buffer (2% SDS, 50 mM Tris-HCl, 10% glycerol, 0.1% Bromphenol blue, pH6.8), washed in 2.5% Triton X-100 for 30 min, then in ddH_2O for 15 min, and incubated at 37 °C overnight in collagenase buffer (50 mM Tris-HCl, 10 mM $CaCl_2$, 200 mM NaCl) supplemented with 0.02% v/v Bruj. Next day, the gel was subjected to Coomassie blue staining/destaining procedure. Negative staining indicates the location of active protease bands. Exposure of pro-enzymes within tissue extracts to SDS during the gel separation procedure leads to activation without proteolytic cleavage.[71]

Histology and immunofluorescence

In all, 10 μm OCT-embedded tissue sections were fixed in 1% paraformaldehyde. The primary antibodies used: anti-mouse VEGF-A (70R-VR001x, Fitzgerald, Acton, MA, USA), anti-Meca-32 (550 563, BD Pharmingen, San Diego, CA, USA), anti-Ki67 (ab16 667, Abcam, Cambridge, UK), anti-murine CD45 (550 539, BD Pharmingen), anti-murine CD4 (14-0042-81, eBioscience, Vienna, Austria), anti-murine Ly-6G (Gr-1) (14-5931-81, eBioscience), phycoerythrin-conjugated CD11b (Mac-1) (557 397, BD Pharmingen), anti-murine CD68 (MCA1957, Serotec, Düsseldorf, Germany), anti-murine F4/80 (MCA497G, Serotec), anti-murine cathepsin B (AF965, R&D Systems, Minneapolis, MN, USA), anti-Glut1 (ab652, Abcam) and anti-murine MMP9 antibodies (gift of Dr Z Werb (UCSF)).

All were applied in blocking buffer (2.5% bovine serum albumin, 5% donkey serum) for 2–16 h. Secondary antibodies were from Dako (Baar, Switzerland) and Molecular Probes (Life Technologies Europe B.V., Zug, Switzerland). Fluorescent images were obtained using Leica DM5500 or, for confocal imagery, Zeiss LSM 700 (PT-BIOP (EPFL)). Immunohistochemical analysis for each antigen was performed at least in duplicate.

Endothelial cell proliferation was quantified in tissue sections by counting randomized fields of endothelial cells (Meca32 +) and calculating the percentage of Ki67 + cells. At least three animals were assayed of each genotype all analyses done in duplicate; 10 randomized fields per analysis were considered. Statistical significance was assessed using the Student's *t*-test. The minimum level of significance was set at $P \leqslant 0.001$.

Analysis of cathepsin activity

The collected tumors were homogenized on ice in lysis buffer (50 mM acetate buffer (pH 5.5), 5 mM dithiothreitol, 5 mM $MgCl_2$, 0.1% Triton X-100). Protein concentration was established by the Bradford assay. The equal amount of protein lysates were labeled with biotinylated DCG-04 ABP[27] for a final concentration 1 μm, equally loaded, separated by SDS-polyacrylamide gel electrophoresis, and transferred onto polyvinylidine fluoride membranes (Roche, Rotkreuz, Switzerland). The cysteine cathepsins activity was determined by incubation with horseradish peroxidase-conjugated streptavidin (Invitrogen, Carlsbad, CA, USA).

Western blot analysis

The tumors were lysed in buffer (50 mM Tris, pH 7.4; 150 mM NaCl, 1% NP-40, 0.1% SDS) containing protease inhibitor (Complete Mini, EDTA-free) and phosphates inhibitors (PhosSTOP) (Roche). Equal amounts of proteins were separated by SDS-polyacrylamide gel electrophoresis and transferred onto polyvinylidine fluoride membranes. Primary antibodies used were as follows: cathepsin B (AF965), cathepsin S (AF1183), cathepsin C (AF1034) (R&D Systems), neutrophil elastase (sc-9521, Santa Cruz, Santa Cruz, CA, USA), anti-β-actin (A2228, Sigma). All secondary antibodies were from Jackson ImmunoResearch Laboratories (West Grove, PA, USA). The quantification of cathepsin expression was determined by Gel Analysis with Fiji package software.

Statistical analysis

Fisher's exact test and the χ^2 test were used to compare tumor invasion metrics via the Prism software package (GraphPad Prism 5 Software, La Jolla, CA, USA). A *P*-value of $P \leqslant 0.02$ was considered significant. Student's *t*-test analysis was used to compare tumor circularity. To compare the profile of inflammatory cells recruited to the tumor sites, a minimum of 35 tumors per group were analyzed. The immune cells were quantified in whole tumor sections and expressed as a percentage of total cells. Student's *t*-test analysis was performed with Prism software package (La Jolla, CA, USA). A *P*-value of $P \leqslant 0.01$ was considered significant.

CONFLICT OF INTEREST

The authors declare no conflict of interest.

ACKNOWLEDGEMENTS

This work was supported by grants from the NCI and by core support from EPLF to DH. KS is a recipient of F32-CA106039. We are extremely grateful to Dr Zena Werb (UCSF) providing the *MMP9-deficient* animal model. Special thanks to Drs Johanna Joyce and Vasilena Gocheva (MSKCC) for providing cathepsin activity probe, antibodies and experimental protocols. We are grateful to Dr Elizabeth Allen and Dr Masahiro Inoue for providing Sutent-treated *RT2* samples and *RT2;RipCre;VEGFA FL/FL* samples, respectively. We are grateful to Drs Lisa Coussens, Luisa Iruela-Arrispe (UCLA), Enrico Giraudo (U of Torino) for helpful discussions and advice. We are grateful to Mr Jeffrey A Kasten (EPFL) for critical reading of the paper. Authors also would like to acknowledge the Bioimaging and Optics platform (PT-*BIOP*) and the Histology Core Facility at EPFL for their services.

REFERENCES

1 Moore MJ, Hamm J, Dancey J, Eisenberg PD, Dagenais M, Fields A *et al.* Comparison of gemcitabine versus the matrix metalloproteinase inhibitor BAY 12-9566 in patients with advanced or metastatic adenocarcinoma of the pancreas: a phase III trial of the National Cancer Institute of Canada Clinical Trials Group. *J Clin Oncol* 2003; **21**: 3296 - 3302.
2 Levin VA, Phuphanich S, Yung WK, Forsyth PA, Maestro RD, Perry JR *et al.* Randomized, double-blind, placebo-controlled trial of marimastat in glioblastoma multiforme patients following surgery and irradiation. *J Neurooncol* 2006; **78**: 295 - 302.
3 Bissett D, O'Byrne KJ, von Pawel J, Gatzemeier U, Price A, Nicolson M *et al.* Phase III study of matrix metalloproteinase inhibitor prinomastat in non-small-cell lung cancer. *J Clin Oncol* 2005; **23**: 842 - 849.
4 Zucker S, Cao J, Chen WT. Critical appraisal of the use of matrix metalloproteinase inhibitors in cancer treatment. *Oncogene* 2000; **19**: 6642 - 6650.
5 Coussens LM, Fingleton B, Matrisian LM. Matrix metalloproteinase inhibitors and cancer: trials and tribulations. *Science* 2002; **295**: 2387 - 2392.
6 Pavlaki M, Zucker S. Matrix metalloproteinase inhibitors (MMPIs): the beginning of phase I or the termination of phase III clinical trials. *Cancer Metastasis Rev* 2003; **22**: 177 - 203.
7 Pellikainen JM, Ropponen KM, Kataja VV, Kellokoski JK, Eskelinen MJ, Kosma VM. Expression of matrix metalloproteinase (MMP)-2 and MMP-9 in breast cancer with

a special reference to activator protein-2, HER2, and prognosis. *Clin Cancer Res* 2004; **10**: 7621 - 7628.
8 Sillanpaa S, Anttila M, Voutilainen K, Ropponen K, Turpeenniemi-Hujanen T, Puistola U *et al.* Prognostic significance of matrix metalloproteinase-9 (MMP-9) in epithelial ovarian cancer. *Gynecol Oncol* 2007; **104**: 296 - 303.
9 Kamat AA, Fletcher M, Gruman LM, Mueller P, Lopez A, Landen Jr CN *et al.* The clinical relevance of stromal matrix metalloproteinase expression in ovarian cancer. *Clin Cancer Res* 2006; **12**: 1707 - 1714.
10 Melchiori A, Albini A, Ray JM, Stetler-Stevenson WG. Inhibition of tumor cell invasion by a highly conserved peptide sequence from the matrix metalloproteinase enzyme prosegment. *Cancer Res* 1992; **52**: 2353 - 2356.
11 Himelstein BP, Canete-Soler R, Bernhard EJ, Dilks DW, Muschel RJ. Metalloproteinases in tumor progression: the contribution of MMP-9. *Invasion Metastasis* 1994; **14**: 246 - 258.
12 Chintala SK, Tonn JC, Rao JS. Matrix metalloproteinases and their biological function in human gliomas. *Int J Dev Neurosci* 1999; **17**: 495 - 502.
13 Bergers G, Brekken R, McMahon G, Vu TH, Itoh T, Tamaki K *et al.* Matrix metalloproteinase-9 triggers the angiogenic switch during carcinogenesis. *Nat Cell Biol* 2000; **2**: 737 - 744.
14 Nozawa H, Chiu C, Hanahan D. Infiltrating neutrophils mediate the initial angiogenic switch in a mouse model of multistage carcinogenesis. *Proc Natl Acad Sci USA* 2006; **103**: 12493 - 12498.
15 Giraudo E, Inoue M, Hanahan D. An amino-bisphosphonate targets MMP-9-expressing macrophages and angiogenesis to impair cervical carcinogenesis. *J Clin Invest* 2004; **114**: 623 - 633.
16 Pahler JC, Tazzyman S, Erez N, Chen YY, Murdoch C, Nozawa H *et al.* Plasticity in tumor-promoting inflammation: impairment of macrophage recruitment evokes a compensatory neutrophil response. *Neoplasia* 2008; **10**: 329 - 340.
17 Du R, Lu KV, Petritsch C, Liu P, Ganss R, Passegue E *et al.* HIF1alpha induces the recruitment of bone marrow-derived vascular modulatory cells to regulate tumor angiogenesis and invasion. *Cancer Cell* 2008; **13**: 206 - 220.
18 Jodele S, Chantrain CF, Blavier L, Lutzko C, Crooks GM, Shimada H *et al.* The contribution of bone marrow-derived cells to the tumor vasculature in neuroblastoma is matrix metalloproteinase-9 dependent. *Cancer Res* 2005; **65**: 3200 - 3208.
19 Yang L, DeBusk LM, Fukuda K, Fingleton B, Green-Jarvis B, Shyr Y *et al.* Expansion of myeloid immune suppressor Gr+CD11b+ cells in tumor-bearing host directly promotes tumor angiogenesis. *Cancer Cell* 2004; **6**: 409 - 421.
20 Pelengaris S, Khan M, Evan GI. Suppression of Myc-induced apoptosis in beta cells exposes multiple oncogenic properties of Myc and triggers carcinogenic progression. *Cell* 2002; **109**: 321 - 334.
21 Shchors K, Shchors E, Rostker F, Lawlor ER, Brown-Swigart L, Evan GI. The Myc-dependent angiogenic switch in tumors is mediated by interleukin 1beta. *Genes Dev* 2006; **20**: 2527 - 2538.
22 Folkman J, Watson K, Ingber D, Hanahan D. Induction of angiogenesis during the transition from hyperplasia to neoplasia. *Nature* 1989; **339**: 58 - 61.
23 Inoue M, Hager JH, Ferrara N, Gerber HP, Hanahan D. VEGF-A has a critical, nonredundant role in angiogenic switching and pancreatic beta cell carcinogenesis. *Cancer Cell* 2002; **1**: 193 - 202.
24 Lawlor ER, Soucek L, Brown-Swigart L, Shchors K, Bialucha CU, Evan GI. Reversible kinetic analysis of Myc targets *in vivo* provides novel insights into Myc-mediated tumorigenesis. *Cancer Res* 2006; **66**: 4591 - 4601.
25 Apte RN, Krelin Y, Song X, Dotan S, Recih E, Elkabets M *et al.* Effects of micro-environment- and malignant cell-derived interleukin-1 in carcinogenesis, tumour invasiveness and tumour-host interactions. *Eur J Cancer* 2006; **42**: 751 - 759.
26 Gocheva V, Wang HW, Gadea BB, Shree T, Hunter KE, Garfall AL *et al.* IL-4 induces cathepsin protease activity in tumor-associated macrophages to promote cancer growth and invasion. *Genes Dev* 2010; **24**: 241 - 255.
27 Joyce JA, Baruch A, Chehade K, Meyer-Morse N, Giraudo E, Tsai FY *et al.* Cathepsin cysteine proteases are effectors of invasive growth and angiogenesis during multistage tumorigenesis. *Cancer Cell* 2004; **5**: 443 - 453.
28 Stetler-Stevenson WG, Aznavoorian S, Liotta LA. Tumor cell interactions with the extracellular matrix during invasion and metastasis. *Annu Rev Cell Biol* 1993; **9**: 541 - 573.
29 van Kempen LC, de Visser KE, Coussens LM. Inflammation, proteases and cancer. *Eur J Cancer* 2006; **42**: 728 - 734.
30 Campbell EJ, Cury JD, Shapiro SD, Goldberg GI, Welgus HG. Neutral proteinases of human mononuclear phagocytes. Cellular differentiation markedly alters cell phenotype for serine proteinases, metalloproteinases, and tissue inhibitor of metalloproteinases. *J Immunol* 1991; **146**: 1286 - 1293.
31 Ahn GO, Brown JM. Matrix metalloproteinase-9 is required for tumor vasculogenesis but not for angiogenesis: role of bone marrow-derived myelomonocytic cells. *Cancer Cell* 2008; **13**: 193 - 205.
32 Dalet-Fumeron V, Guinec N, Pagano M. *In vitro* activation of pro-cathepsin B by three serine proteinases: leucocyte elastase, cathepsin G, and the urokinase-type plasminogen activator. *FEBS Lett* 1993; **332**: 251 - 254.
33 Geraghty P, Rogan MP, Greene CM, Boxio RM, Poiriert T, O'Mahony M *et al.* Neutrophil elastase up-regulates cathepsin B and matrix metalloprotease-2 expression. *J Immunol* 2007; **178**: 5871 - 5878.
34 Kruger A, Soeltl R, Sopov I, Kopitz C, Arlt M, Magdolen V *et al.* Hydroxamate-type matrix metalloproteinase inhibitor batimastat promotes liver metastasis. *Cancer Res* 2001; **61**: 1272 - 1275.
35 Overall CM, Kleifeld O. Tumour microenvironment - opinion: validating matrix metalloproteinases as drug targets and anti-targets for cancer therapy. *Nat Rev Cancer* 2006; **6**: 227 - 239.
36 Coussens LM, Tinkle CL, Hanahan D, Werb Z. MMP-9 supplied by bone marrow-derived cells contributes to skin carcinogenesis. *Cell* 2000; **103**: 481 - 490.
37 Littlepage LE, Sternlicht MD, Rougier N, Phillips J, Gallo E, Yu Y *et al.* Matrix metalloproteinases contribute distinct roles in neuroendocrine prostate carcinogenesis, metastasis, and angiogenesis progression. *Cancer Res* 2010; **70**: 2224 - 2234.
38 Himelstein BP, Lee EJ, Sato H, Seiki M, Muschel RJ. Transcriptional activation of the matrix metalloproteinase-9 gene in an H-ras and v-myc transformed rat embryo cell line. *Oncogene* 1997; **14**: 1995 - 1998.
39 Chesler L, Goldenberg DD, Seales IT, Satchi-Fainaro R, Grimmer M, Collins R *et al.* Malignant progression and blockade of angiogenesis in a murine transgenic model of neuroblastoma. *Cancer Res* 2007; **67**: 9435 - 9442.
40 Sekhon HS, London CA, Sekhon M, Iversen PL, Devi GR. c-MYC antisense phosphosphorodiamidate morpholino oligomer inhibits lung metastasis in a murine tumor model. *Lung Cancer* 2008; **60**: 347 - 354.
41 Elaraj DM, Weinreich DM, Varghese S, Puhlmann M, Hewitt SM, Carroll NM *et al.* The role of interleukin 1 in growth and metastasis of human cancer xenografts. *Clin Cancer Res* 2006; **12**: 1088 - 1096.
42 Voronov E, Shouval DS, Krelin Y, Cagnano E, Benharroch D, Iwakura Y *et al.* IL-1 is required for tumor invasiveness and angiogenesis. *Proc Natl Acad Sci USA* 2003; **100**: 2645 - 2650.
43 Lee HT, Lee JG, Na M, Kay EP. FGF-2 induced by interleukin-1 beta through the action of phosphatidylinositol 3-kinase mediates endothelial mesenchymal transformation in corneal endothelial cells. *J Biol Chem* 2004; **279**: 32325 - 32332.
44 Lockwood CJ, Matta P, Krikun G, Koopman LA, Masch R, Toti P *et al.* Regulation of monocyte chemoattractant protein-1 expression by tumor necrosis factor-alpha and interleukin-1beta in first trimester human decidual cells: implications for preeclampsia. *Am J Pathol* 2006; **168**: 445 - 452.
45 Raymond L, Eck S, Mollmark J, Hays E, Tomek I, Kantor S *et al.* Interleukin-1 beta induction of matrix metalloproteinase-1 transcription in chondrocytes requires ERK-dependent activation of CCAAT enhancer-binding protein-beta. *J Cell Physiol* 2006; **207**: 683 - 688.
46 Mountain DJ, Singh M, Menon B, Singh K. Interleukin-1beta increases expression and activity of matrix metalloproteinase-2 in cardiac microvascular endothelial cells: role of PKCalpha/beta1 and MAPKs. *Am J Physiol Cell Physiol* 2007; **292**: C867 - C875.
47 Deryugina EI, Quigley JP. Pleiotropic roles of matrix metalloproteinases in tumor angiogenesis: contrasting, overlapping and compensatory functions. *Biochim Biophys Acta* 2010; **1803**: 103 - 120.
48 Tazawa H, Okada F, Kobayashi T, Tada M, Mori Y, Une Y *et al.* Infiltration of neutrophils is required for acquisition of metastatic phenotype of benign murine fibrosarcoma cells: implication of inflammation-associated carcinogenesis and tumor progression. *Am J Pathol* 2003; **163**: 2221 - 2232.
49 Shojaei F, Wu X, Malik AK, Zhong C, Baldwin ME, Schanz S *et al.* Tumor refractoriness to anti-VEGF treatment is mediated by CD11b+Gr1+ myeloid cells. *Nat Biotechnol* 2007; **25**: 911 - 920.
50 Yang L, Huang J, Ren X, Gorska AE, Chytil A, Aakre M *et al.* Abrogation of TGF beta signaling in mammary carcinomas recruits Gr-1+CD11b+ myeloid cells that promote metastasis. *Cancer Cell* 2008; **13**: 23 - 35.
51 Ebos JM, Lee CR, Cruz-Munoz W, Bjarnason GA, Christensen JG, Kerbel RS. Accelerated metastasis after short-term treatment with a potent inhibitor of tumor angiogenesis. *Cancer Cell* 2009; **15**: 232 - 239.
52 Paez-Ribes M, Allen E, Hudock J, Takeda T, Okuyama H, Vinals F *et al.* Antiangiogenic therapy elicits malignant progression of tumors to increased local invasion and distant metastasis. *Cancer Cell* 2009; **15**: 220 - 231.
53 Balbin M, Fueyo A, Tester AM, Pendas AM, Pitiot AS, Astudillo A *et al.* Loss of collagenase-2 confers increased skin tumor susceptibility to male mice. *Nat Genet* 2003; **35**: 252 - 257.
54 McCawley LJ, Wright J, LaFleur BJ, Crawford HC, Matrisian LM. Keratinocyte expression of MMP3 enhances differentiation and prevents tumor establishment. *Am J Pathol* 2008; **173**: 1528 - 1539.

55 Turk V, Turk B, Guncar G, Turk D, Kos J. Lysosomal cathepsins: structure, role in antigen processing and presentation, and cancer. *Adv Enzyme Regul* 2002; **42**: 285 - 303.
56 Turk V, Turk B, Turk D. Lysosomal cysteine proteases: facts and opportunities. *EMBO J* 2001; **20**: 4629 - 4633.
57 Gocheva V, Joyce JA. Cysteine cathepsins and the cutting edge of cancer invasion. *Cell Cycle* 2007; **6**: 60 - 64.
58 Grimm J, Kirsch DG, Windsor SD, Kim CF, Santiago PM, Ntziachristos V *et al.* Use of gene expression profiling to direct *in vivo* molecular imaging of lung cancer. *Proc Natl Acad Sci USA* 2005; **102**: 14404 - 14409.
59 Gocheva V, Zeng W, Ke D, Klimstra D, Reinheckel T, Peters C *et al.* Distinct roles for cysteine cathepsin genes in multistage tumorigenesis. *Genes Dev* 2006; **20**: 543 - 556.
60 Lah TT, Buck MR, Honn KV, Crissman JD, Rao NC, Liotta LA *et al.* Degradation of laminin by human tumor cathepsin B. *Clin Exp Metastasis* 1989; **7**: 461 - 468.
61 Buck MR, Karustis DG, Day NA, Honn KV, Sloane BF. Degradation of extracellular-matrix proteins by human cathepsin B from normal and tumour tissues. *Biochem J* 1992; **282** (Part 1):273 - 278.
62 Creemers LB, Hoeben KA, Jansen DC, Buttle DJ, Beertsen W, Everts V. Participation of intracellular cysteine proteinases, in particular cathepsin B, in degradation of collagen in periosteal tissue explants. *Matrix Biol* 1998; **16**: 575 - 584.
63 Levicar N, Nuttall RK, Lah TT. Proteases in brain tumour progression. *Acta Neurochir* 2003; **145**: 825 - 838.
64 Czyzewska J, Guzinska-Ustymowicz K, Kemona A, Bandurski R. The expression of matrix metalloproteinase 9 and cathepsin B in gastric carcinoma is associated with lymph node metastasis, but not with postoperative survival. *Folia Histochem Cytobiol* 2008; **46**: 57 - 64.
65 Kirschke H, Clausen T, Gohring B, Gunther D, Heucke E, Laube F *et al.* Concentrations of lysosomal cysteine proteases are decreased in renal cell carcinoma compared with normal kidney. *J Cancer Res Clin Oncol* 1997; **123**: 402 - 406.
66 Batist G, Patenaude F, Champagne P, Croteau D, Levinton C, Hariton C *et al.* Neovastat (AE-941) in refractory renal cell carcinoma patients: report of a phase II trial with two dose levels. *Ann Oncol* 2002; **13**: 1259 - 1263.
67 Lopez T, Hanahan D. Elevated levels of IGF-1 receptor convey invasive and metastatic capability in a mouse model of pancreatic islet tumorigenesis. *Cancer Cell* 2002; **1**: 339 - 353.
68 Chun MG, Mao JH, Chiu CW, Balmain A, Hanahan D. Polymorphic genetic control of tumor invasion in a mouse model of pancreatic neuroendocrine carcinogenesis. *Proc Natl Acad Sci USA* 2010; **107**: 17268 - 17273.
69 Sounni NE, Dehne K, van Kempen L, Egeblad M, Affara NI, Cuevas I *et al.* Stromal regulation of vessel stability by MMP14 and TGFbeta. *Dis Model Mech* 2010; **3**: 317 - 332.
70 Herron GS, Banda MJ, Clark EJ, Gavrilovic J, Werb Z. Secretion of metalloproteinases by stimulated capillary endothelial cells. II. Expression of collagenase and stromelysin activities is regulated by endogenous inhibitors. *J Biol Chem* 1986; **261**: 2814 - 2818.
71 Herron GS, Werb Z, Dwyer K, Banda MJ. Secretion of metalloproteinases by stimulated capillary endothelial cells. I. Production of procollagenase and prostromelysin exceeds expression of proteolytic activity. *J Biol Chem* 1986; **261**: 2810 - 2813.

Supplementary Information accompanies the paper on the Oncogene website (http://www.nature.com/onc)